Design and Characterization of a Variable-Length Piezocomposite Transducer for Structural Health Monitoring

Ken I. Salas and Carlos E.S. Cesnik

Journal of Intelligent Material Systems and Structures 2010 21: 349 originally published online 6 August 2009
DOI: 10.1177/1045389X09343219

Design and Characterization of a Variable-Length Piezocomposite Transducer for Structural Health Monitoring

KEN I. SALAS AND CARLOS E. S. CESNIK*

Department of Aerospace Engineering, The University of Michigan
1320 Beal Avenue, Ann Arbor, MI 48109-2140, USA

ABSTRACT: A modally selective, variable-length anisotropic piezocomposite transducer is designed for guided wave (GW) structural health monitoring applications. The transducer dimensions needed to maximize individual modes are selected based on 3D elasticity models for GW excitation by finite dimensional transducers. This theory is used to determine these transducer dimensions as a function of the wave phase velocity, and normalized by the substrate thickness. The design and fabrication of the transducer are subsequently described, and a set of experimental tests is conducted in pristine isotropic structures to characterize the actuation and sensing performance of the device. It is shown that the transducer dimensions can be tailored to obtain specific symmetric to antisymmetric mode transmission and sensing ratios.

Key Words: structural health monitoring, piezoelectric, sensor, actuator, quided waves, piezocomposit transducer, model selectivity, variable-length.

INTRODUCTION

STRUCTURAL health monitoring (SHM) is the component of damage prognosis systems responsible for interrogating a structural component to detect the presence and location of defects. Guided wave (GW) testing methods have gained attention for SHM systems due to several of their attractive features. The reader is referred to the work of Raghavan and Cesnik (2007a) for a comprehensive review of this field. In addition to their ability to propagate long distances with small attenuation, GWs can be made sensitive to specific damage types. This feature can be controlled based on the excitation frequency and transducer geometry. In the excitation of GWs using finite dimensional transducers, there are two main contributions to the induced displacements or strains. The first of these, which is typically referred to as the excitability function, is primarily dependent on the substrate under inspection. That is, for a given set of material properties and geometry, there will be frequencies at which displacements from specific GW modes will be maximized. This fact, along with dispersion considerations, is typically used to determine the excitation frequency to be used. The second component is related to the transducer geometry and size. These parameters can be selected so that they are most effective at exciting specific GW modes (this is done according to the wavelength of the desired mode as discussed later).

The idea of variable-length devices has received little attention in the past, with some efforts directed towards the design of phased array and comb-arrays of transducers (e.g., Pelts et al., 1996). The work of Monkhouse et al. (1997, 2000) explored this idea by developing an interdigital polyvinylidene fluoride (PVDF) transducer to excite specific GW modes. The main criterion used in sizing the device was to operate at points of minimal dispersion. Because of the nature of the active material, the variable length was controlled by changing the width and spacing of the electrode fingers. It is well known, however, that PVDF is not well suited for SHM applications because of its weak sensor response. Due to their strong piezoelectric coupling (based on the 3-3 effect), actuation directionality, and flexibility anisotropic piezocomposite transducers (APT) are an attractive option for GW transduction in SHM systems. In this study, a rectangular variable-length APT, capable of exciting specific GW modes, is designed and tested with applications to SHM. This represents a first step towards the implementation of modal selectivity in transducer arrays such as the CLoVER transducer previously introduced by the authors (Salas and Cesnik, 2008a). The transducer is based on the NASA macro-fiber-composite (MFC) actuator developed by Wilkie and High (2003), and is composed of piezoceramic fibers embedded in a structural epoxy. The excitation voltage is provided through interdigitated electrodes that surround the device. The variable-length effect is

*Author to whom correspondence should be addressed.
E-mail: cesnik@umich.edu
Figures 1–7 and 9–19 appear in color online: http://jim.sagepub.com

1045-389X/10/03 0349–12 $10.00/0 DOI: 10.1177/1045389X09343219

achieved by designing the electrode pattern so that it has independent subdivisions or segments. These can be activated using a multiplexing unit and a suitable control algorithm.

There are multiple potential benefits in using variable-length devices for GW transduction. The first, and likely most important, benefit is the potential ability to selectively excite and sense individual modes. This would be advantageous as the propagating pulse could be specifically designed to be sensitive to different damage types. Conversely, using a sensor able to predominantly receive contributions from specific modes, while minimizing those from undesired ones, would greatly facilitate the processing of inspection signals. Similarly, a variable-length transducer can potentially have the ability to operate at points of low dispersion in the frequency-thickness domain to ensure that the different frequency components do not separate as the pulse propagates through the structure under inspection. This is advantageous as it maintains the signal-to-noise ratio and facilitates the processing of reflections from closely spaced features as discussed by Monkhouse et al. (2000) and Alleyne and Cawley (1992).

Another important potential benefit is the ability for environmental compensation. The transducer dimensions necessary to obtain a specific mode ratio are likely to be selected for a specific set of operating conditions, that is, specific temperature, loading, and material conditions, all of which may change while the structure is in operation. Consider for instance the effect of temperature. This parameter is of crucial importance for GW propagation and damage detection, and its effects have addressed by several researchers in the past (e.g., Konstantinidis et al., 2006; Raghavan and Cesnik, 2007b; Clarke and Cawley, 2008). While the primary complications arise due to the influence of temperature on baseline signals typically used for damage detection and localization, GW transduction is also affected due to the changing transducer material properties and bond-line conditions. Furthermore, the mechanical loads acting on the substrate can also influence its wave propagation properties. For instance, the work of Chen and Wilcox (2007) showed that for the fundamental antisymmetric (A_0) mode in an aluminum plate, the phase velocity increased by a factor of as much as four under strain levels of 0.1% for frequency-thickness products of up to 10 kHz mm. This effect would directly influence the transducer dimension as it typically depends on the mode wavelength, itself a function of the phase velocity. Finally, in the case of anisotropic structures the transducer dimensions will be dependent on the inspection direction. This effect can be observed in Figure 1, which shows the directional dependence of the fundamental symmetric (S_0) mode wavelength in a 4-layer IM7-based cross-ply laminate at 200 kHz. These results were generated using the

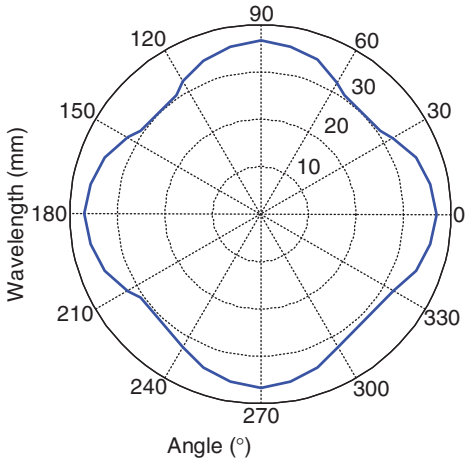

Figure 1. *Directional dependence of S_0 mode wavelength at 200 kHz on 4-layer $[0/90]_S$ cross-ply laminated composite plate.*

software *Disperse* v2.0.16d developed at Imperial College, UK (Pavlakovic and Lowe, 2007). As the transducer dimensions are based on the wavelength, it is clear that its value should change with angular position so as to maintain a constant mode transmission and sensing ratio. For typical applications of the GW approach for damage detection in composite materials, the reader is referred to the work of Diamanti and Soutis (2004, 2005, 2007).

The theoretical background for GW excitation that will be used to determine the optimal transducer dimensions is briefly discussed next, and an expression for the transducer dimension that maximizes the transmission of a specific mode is presented. The criteria for the design of the transducer are subsequently described, along with a brief overview of its fabrication procedure. A set of experimental studies are later presented to illustrate the ability of the device to attain specific mode transmission and sensing ratios.

THEORETICAL BACKGROUND

The transducer dimensions in each variable-length device are selected so as to maximize the transmission and excitation purity of the S_0 or A_0 modes at different frequencies. These dimensions are obtained from the theory developed by Raghavan and Cesnik (2007c) for GW excitation by a rectangular, finite-dimensional piezocomposite transducer in isotropic plates. Their theoretical model is based on the 3D equations of elasticity and is based on assuming uncoupled dynamics and perfect bond between the transducer and substrate. These assumptions result in the interaction between the substrate and the actuator being represented through shear tractions along the edges of the transducer in the piezoceramic fiber direction, as shown in Figure 2. It was shown by Crawley and de Luis (1987) that if these conditions are not satisfied, a shear-lag solution accounting

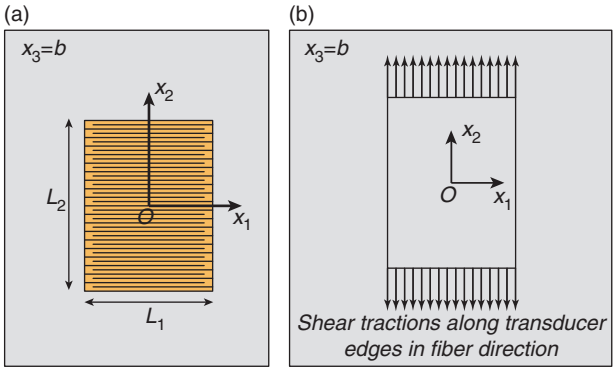

Figure 2. *(a) Piezocomposite transducer bonded on the surface of the specimen (note that the horizontal lines represent the electrode pattern and that the fibers are aligned with the x_2-direction); (b) The transducer is modeled as shear tractions along its edges on the surface of the substrate.*

for the thickness of the bond-line is necessary for accurate results. Nevertheless, the fitness of these assumptions in the theoretical modeling of GW excitation by these transducers has been numerically and experimentally verified in previous studies (Raghavan and Cesnik, 2005; Salas and Cesnik, 2009). Under the above assumptions, the equilibrium equations expressed in displacement form are solved using Fourier transforms and complex calculus under the set of boundary conditions given by Equation (1), from which the dependence of the induced GW field on the transducer dimensions can be derived.

$$\begin{aligned}
&\sigma_{31}(x_3 = b) = 0 \\
&\sigma_{32}(x_3 = b) = \tau_0\left[u\left(x_1 - \frac{L_1}{2}\right) - u\left(x_1 + \frac{L_1}{2}\right)\right] \\
&\qquad\qquad \left[\delta\left(x_2 - \frac{L_2}{2}\right) - \delta\left(x_2 + \frac{L_2}{2}\right)\right] \\
&\sigma_{33}(x_3 = b) = 0
\end{aligned} \tag{1}$$

In Equation (1) σ_{ij} corresponds to the stress components, b represents the substrate half-thickness ($t = 2b$), τ_0 represents the traction amplitude, $u(.)$ corresponds to the unit step function, and $\delta(.)$ represents the Dirac delta function. Similarly, L_1 and L_2 represent the transducer dimensions along the x_1- and x_2-directions, respectively. The results from this theory have been extensively verified numerically and experimentally, and good correlation has been obtained in the time, frequency, and space domains (Raghavan and Cesnik, 2005; Salas and Cesnik, 2008b). For the case of a rectangular APT with the fibers oriented along the x_2-direction (the direction where the displacements are to be maximized), as depicted in Figure 2, it can be shown that the transducer dimension should be selected based on the result given in Equation (2):

$$\sin \xi \frac{L_2}{2} = 1 \tag{2}$$

where ξ corresponds to the wavenumber of the mode under consideration. From Equation (2) it follows that the transducer dimensions that maximize the displacements at a given frequency, a^*, should be selected as (Raghavan and Cesnik, 2007c):

$$a^* = \left(n + \frac{1}{2}\right)\frac{2\pi}{\xi} \tag{3}$$

where n represents an integer ($n = 0, 1, 2, \ldots$). The necessary wavenumber in Equation (3) is obtained from the dispersion relation for either the S_0 or A_0 mode which, for the antisymmetric case, is given by:

$$D_A = (\xi^2 - \beta^2)^2 \sin \alpha b \cos \beta b + 4\xi^2 \alpha\beta \cos \alpha b \sin \beta b \tag{4}$$

where the terms a and β represent through-the-thickness wavenumbers (Raghavan and Cesnik, 2005). Equation (3) can be expressed in terms of the mode wavelength, λ, by using the equality $\lambda = 2\pi/\xi$, so that the desired transducer dimension is expressed as:

$$a^* = (2n + 1)\frac{\lambda}{2} \tag{5}$$

The result given by Equation (3) can then be generalized for a substrate of any thickness by using the definition of the phase velocity, c_p, which is known to be a function of the frequency-thickness product, ft (Graff, 1991):

$$c_p = \frac{\omega}{\xi} = \frac{2\pi f}{\xi} = \text{function}(ft) \tag{6}$$

By substituting the definition in Equation (6) into the result obtained in Equation (3) one finds:

$$a^* = (2n + 1)\frac{c_p(ft)}{2f} \tag{7}$$

where the parentheses in the c_p term indicate that this variable is a function of the frequency-thickness product, ft. Finally, dividing both sides by the substrate thickness, t, and defining $\chi = ft$ results in:

$$\frac{a^*}{t} = (2n + 1)\frac{c_p(ft)}{2ft} = (2n + 1)\frac{c_p(\chi)}{2\chi} \tag{8}$$

Sample results from Equation (8) are shown in Figure 3, which shows the transducer dimension that maximizes the transmission of the A_0 mode in an aluminum plate ($E = 70\,\text{GPa}$, $\nu = 0.33$, $\rho = 2700\,\text{kg/m}^3$). Note that the dimensions that result in no transmission of a specific mode can be found analogously by setting the right-hand side of Equation (2) equal to zero.

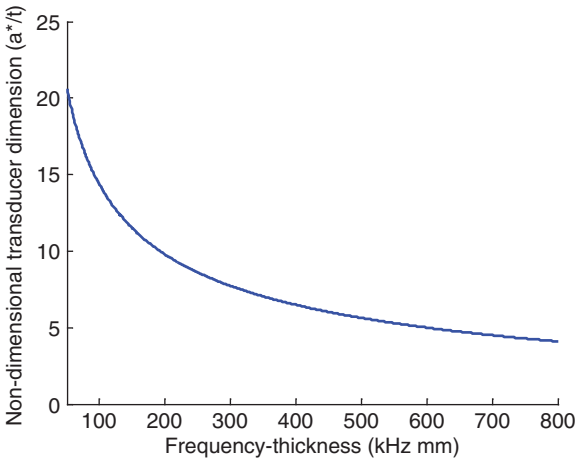

Figure 3. *Transducer dimensions normalized by substrate thickness needed to maximize A_0 mode transmission in aluminum 5005 plate.*

Denoting this transducer dimension by o^*, it can be expressed as:

$$\frac{o^*}{t} = n\frac{c_p(\chi)}{\chi} \tag{9}$$

where, as in the previous case, n represents an integer number. In the following section, the results in Equations (8) and (9) are used to select the transducer dimensions so that the transmission of a specific mode is maximized, while that of the opposite mode is minimized.

TRANSDUCER DESIGN AND FABRICATION

Brief Background on Piezocomposite Transducers

Piezocomposite transducers have been introduced over the past decade as an alternative transduction concept over monolithic piezoelectric wafers. These devices possess multiple advantages over conventional wafers. First, due to their composite construction, they have enhanced flexibility, which allows them to be easily attached to curved surfaces. Similarly, due to their construction, these devices operate on the 3-3 piezoelectric effect, where the electric field and primary strain direction are parallel. This feature gives the transducers a higher strain energy density, theoretically allowing them to produce strains as large as two times those attainable with conventional piezoelectric wafers. Finally, the structural epoxy and polymer casing provide additional protection to the ceramic from damage due to environmental conditions, and give them a higher specific strength relative to conventional wafers.

The first such transducer, termed Active Fiber Composite, was introduced by Bent and Hagood (1995) and was composed of cylindrical extruded fibers embedded in a structural epoxy and surrounded by interdigitated electrodes for actuation. Wilkie and High (2003) developed an alternative concept, the MFC, which was composed of prismatic fibers with a rectangular cross-section obtained from dicing piezoelectric sheets using computer-controlled dicing saws. Prior to the dicing procedure, the piezoceramic sheets were attached to an adhesive carrier film, which allowed the resulting fibers to be handled as a bundle. This facilitates their uniform alignment relative to the electrode pattern. A comprehensive study on the electromechanical properties of these devices can be found in the work by Williams (2004).

Transducer Design

Several important parameters must be considered during the selection of the dimension of each segment in the variable-length transducer. First, the mode transmission ratio (defined as the ratio of the peak-to-peak amplitude of the propagating S_0–A_0 modes, S_0/A_0) must be considered so that each dimension is able to selectively excite either the symmetric or antisymmetric mode. Ideally, the transducer would be sized at a point where one mode has a peak, while the opposite mode has a minimum. As Figures 4 and 5 show, there are a small number of points in the frequency-thickness domain where this can be exactly achieved. Note that the results shown correspond to an aluminum 5005 alloy ($E = 68.9$ GPa, $\nu = 0.33$, $\rho = 2700$ kg/m^3), but similar results are expected for other isotropic material systems. It should be noted that, as seen in Figures 4 and 5, for low frequency-thickness products (<100 kHz mm for the material parameters considered here), this requires a large transducer dimension (in the order of 30 times the substrate thickness for the symmetric mode and larger than 40 times the substrate thickness for the antisymmetric mode for the material parameters considered), which is not desirable based on power-consumption and implementation considerations.

The second important parameter is the wavelength range desired in order to have large sensitivity to different defect sizes. Previous studies have shown that the reflection amplitude from defects can be correlated to the ratio of the wavelength to a defect characteristic dimension. For instance, in Lowe et al. (2002), the interaction of the fundamental Lamb modes with part-depth notches was studied through finite element analysis and experimental measurements. Their results indicated that for relatively shallow notches (<15% of the substrate thickness), the reflection amplitude was maximized if the S_0 mode wavelength was equal to four times the defect diameter, or if the A_0 mode wavelength was equal to two times the defect diameter. Similar correlations have been found for different defect types and depths (Diligent and Lowe, 2005; Fromme et al., 2004).

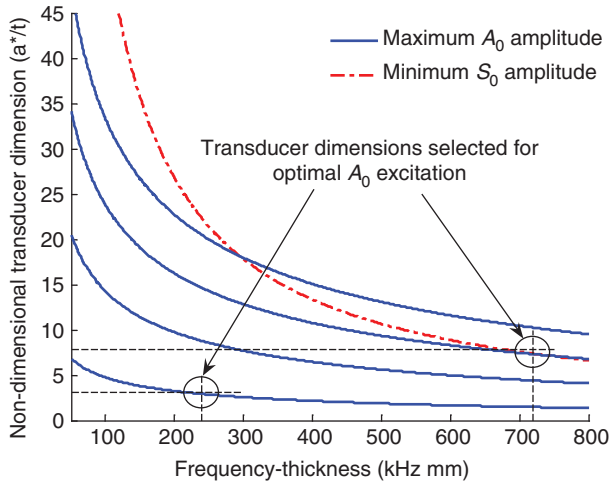

Figure 4. *Transducer dimensions selected to maximize A_0 mode transmission at 240 kHz mm and 720 kHz mm.*

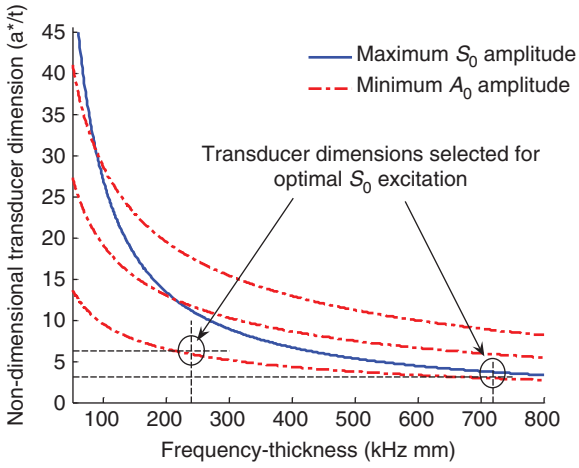

Figure 5. *Transducer dimensions selected to maximize S_0 mode transmission at 240 kHz mm and 720 kHz mm.*

The mode wavelength is a function of the material properties and thickness of the substrate under consideration as well as the testing frequency, and therefore the desired range needs to be selected on a case-by-case basis.

The transducer dimensions selected in this study, along with the expected mode transmission ratios expected at two frequency-thickness products of interest are summarized in Table 1, and illustrated in Figures 4 and 5. Note that the dimensions selected are expected to produce large transmission ratios for each mode at two different points, and that the mode ratios indicated are based only on Equations (8) and (9) and do not account for the different substrate excitability at different frequency-thickness ranges. The actual frequencies based on a 3.2-mm aluminum plate were selected as they produced a range of wavelengths that will be useful in damage detection experiments. These wavelengths are summarized in Table 2.

Table 1. Summary of transducer dimensions and mode transmission ratios available in variable-length APT.

Transducer dimension (mm)	S_0/A_0 at 240 (kHz mm)	S_0/A_0 at 720 (kHz mm)
10	0.4	5
20	4	–
25	–	~0

Table 2. Mode wavelengths at design frequencies for variable-length APT.

Frequency (kHz)	S_0 wavelength (mm)	A_0 wavelength (mm)
75	71.3	18.7
225	23.6	9.4

In the case of the symmetric mode at 240 kHz-mm, the dimension was chosen so as to minimize the A_0 transmission without maximizing the S_0 mode as this would require a larger transducer, as seen in Figure 6. Similarly, in the case of the antisymmetric mode at the same frequency-thickness the dimension selected maximizes the A_0 transmission without minimizing the S_0 amplitude as this would result in an even larger device. Finally, Figure 7 shows that, due to the smaller wavelengths, the dimensions selected at 720 kHz mm maximize one mode transmission, while minimizing that of the other mode. Finally, it is important to mention that the transducer dimensions selected are expected to provide similar transmission ratios for neighboring frequencies as well.

Based on the dimensions discussed above, the interdigitated electrode pattern shown in Figure 8 was designed to attain the variable-length effect. It can be seen that each subdivision is connected to a separate electrode bus for independent actuation. In addition, for future damage detection tests in pulse-echo mode, a dedicated sensor element has been added to the pattern in a manner such that the defect reflections will not interact with the actuator elements. Also note that the tabs for wire lead connections have been placed on the sides of the device, which decreases the transducer disturbance to the GW field. The specific parameters in the electrode pattern were selected based on those of the NASA-standard MFC devices (Wilkie and High, 2003). In particular, the finger width was selected at 0.1 mm, while the finger spacing was chosen as 0.5 mm. The electrode pattern was transferred to a copper-clad kapton film (Pyralux LF7062R) using a photolithography process at the Lurie Nanofabrication Facility at the University of Michigan. There was no specific criterion followed to select the width of the device, other than to maintain a value within acceptable bounds. This dimension is only expected to scale the

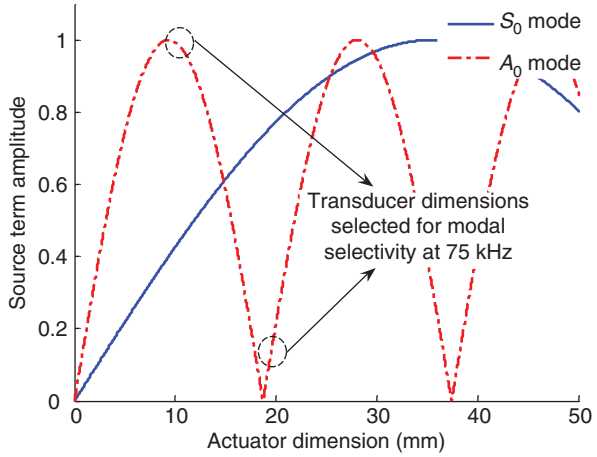

Figure 6. *Ratio of S_0 to A_0 transmission for the different transducer dimensions selected at 75 kHz.*

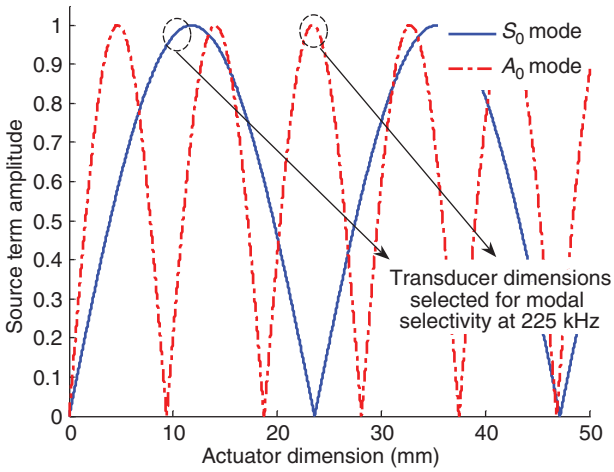

Figure 7. *Ratio of S_0 to A_0 transmission for the different transducer dimensions selected at 225 kHz.*

amplitude of the strains induced or sensed by the transducer, and to have no effect in the trends observed for the transducer as the piezoelectric properties of the device are very weak along this direction. As previously indicated, the dimension along the length of the piezoelectric fibers is the critical dimension to control in these transducers.

The construction of the devices used in this study is based on the MFC transducer. The piezoelectric material used in this case was PZT-5A, which had a thickness of 0.2 mm. A pristine ceramic sheet was diced into rectangular fibers with a width of 0.3 mm and an inter-fiber spacing of ~0.05 mm. The length and width of the fiber sheet was selected to match the dimensions of the electrode pattern. The structural epoxy used for bonding the fibers and the electrode patterns was Loctite E-120HP for consistency with the material system used in the standard fabrication procedure (Wilkie and High, 2003). The assembly of the transducer was performed according to the NASA-standard fabrication procedure for MFC

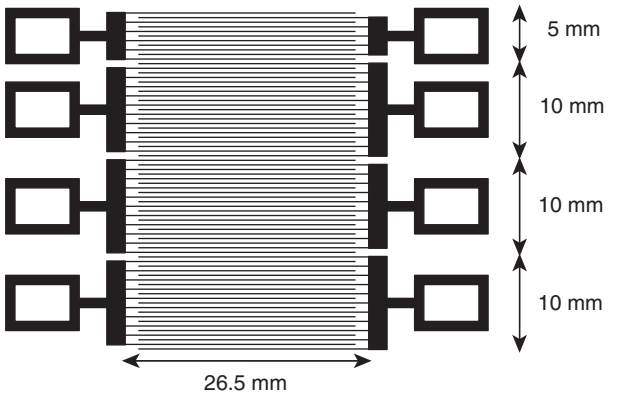

Figure 8. *Interdigitated electrode pattern used in variable-length APT.*

transducers (Wilkie and High, 2003), while the cure of the device was performed following an adaptation of that procedure previously used by the authors (Salas and Cesnik, 2008a). In particular, a piezoceramic sheet with the dimensions mentioned earlier was diced into fibers, which were held together by an adhesive carrier film. The entire fiber bundle was subsequently aligned with the electrode patterns so that the resulting electric field was oriented along the length of the fibers. The poling of the devices was conducted at an electric field of 2.4 kV/mm (assuming the electric field acted over the nominal interdigitated electrode separation distance), at a temperature of 90°C for 30 min. This process has been shown to produce transducers with a free strain performance consistent with that of NASA-standard devices (Salas and Cesnik, 2008a). In the study by Williams (2004), it was shown that typical piezocomposite transducers fabricated using the NASA-standard manufacturing procedure had a fiber volume fraction in the order of 0.9. As all assembly procedures and the free-strain performance of the resulting devices were consistent with the NASA-standard, the volume fraction of the actuators developed is expected to be of a similar order.

EXPERIMENTAL SETUP

The variable-length APT was bonded on a 3.2-mm thick aluminum 5005 plate at its geometric center using a thin layer of Epotek 730 bonding agent. The in-plane dimensions of the square plate were 0.7 m on each side. It is important that the bond-line between the transducer and the substrate be as thin as possible to ensure that shear-lag effects can be neglected (Crawley and de Luis, 1987). If the bonding line is excessively thick the strains from the actuator will be transferred to the substrate over a finite distance along its length instead of at its edges. This would in turn result in the effective dimension of the transducer being smaller than its nominal dimension. In order to ensure that a thin and uniform bond line was obtained, the transducer and

plate were placed in an autoclave and cured for 2 h at a temperature of 80°C (according to the manufacturer instructions) and pressure of 345 kPa (50 psi). This procedure was observed to yield the thinnest possible bond line without the risk of causing damage to the device due to excessive pressure, and has been previously shown to produce bonding layers that satisfy the perfect-bonding assumption (Raghavan and Cesnik, 2005; Salas and Cesnik, 2009). To characterize the transduction properties of the variable-length device a combination of laser vibrometer and sensor-based measurements were collected. The experimental details and results for each of these are presented in the following subsections.

Laser Vibrometer Experiments

The objective of these tests was to obtain a detailed characterization of the antisymmetric mode in near-harmonic excitation conditions, which is expected to result in a closer correlation with the expected results from the selection of the transducer dimensions (calculated using a single frequency component). As a result, a Polytec PSV-400 scanning laser vibrometer, sensitive to the out-of-plane velocities of the specimen under inspection, was used. This device operates under the Doppler shifting phenomenon and uses a Helium-Neon laser beam ~60 μm in diameter at the used standoff distance (915 mm between the laser scanning head and the plate) (Polytec, 2007). As the symmetric out-of-plane displacement and velocity components are very weak at lower frequencies (below ~300 kHz), the laser is mostly sensitive to the antisymmetric mode.

In an effort to excite the transducer with a single frequency component, a 10-cycle sinusoidal function was used as the excitation signal. An Agilent 33220A arbitrary waveform generator was used in conjunction with a Trek PZD2000 high power amplifier for this purpose. The acquisition frequency used with the laser vibrometer was 5.12 MHz. An overview of the experimental setup is shown in Figure 9. The peak-to-peak input voltage to each APT segment was in the order of 500 V (somewhat larger voltages were used at higher frequencies to compensate for the decreasing amplifier gain). The wavelength for each of the frequencies tested was different, being larger for the lower frequencies. It is well known that the amplitude attenuation of GWs is a function of the propagation distance relative to the mode wavelength. Therefore, multiple measurement points were selected so as to always collect signals at a normalized distance of three wavelengths away from the edge of the transducer. Previous work by the authors has shown good correlation with experiments by considering this location as the source of the propagating GWs (Salas and Cesnik, 2008b). A summary of these positions is presented in Figure 10, where they range from 103 mm for 25 kHz to 28 mm for 250 kHz. The peak-to-peak amplitude of the recorded pulses was used as the metric in this case.

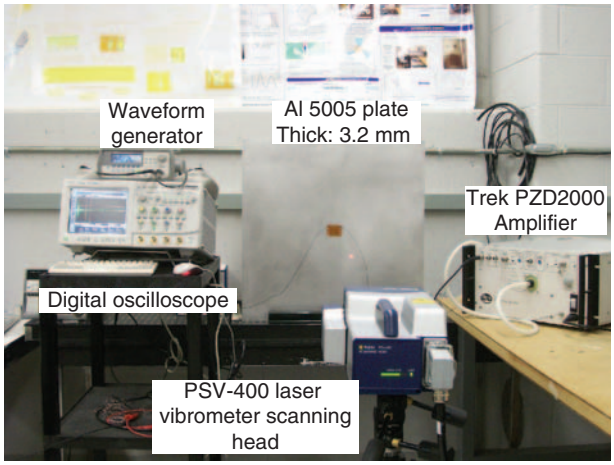

Figure 9. *Overview of experimental setup used in laser vibrometer experiments.*

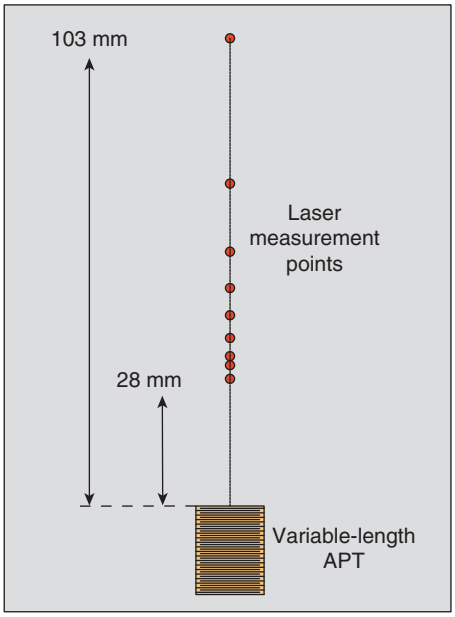

Figure 10. *Schematic of laser vibrometer monitoring points.*

Sample results from these experiments are shown in Figures 11 and 12. Figure 11 shows a sample time domain signal recorded with the laser vibrometer. All the measurements presented subsequently were made between the fourth and seventh propagating pulses. Each measurement was averaged a total of 64 times and three separate measurements were collected at each testing frequency. The peak-to-peak amplitude for each segment in the variable-length device is shown in Figure 12, where the error bars represent three times the standard deviation.

Several important observations can be made from these results. First, note that for the 10- and 25-mm segments the peaks occur at 100 kHz in contrast to the

20-mm segment, where the peak occurs at 125 kHz. This is directly related to the ratio of the transducer dimension to the mode wavelength. At 100 kHz, the A_0 mode has a wavelength of ~16 mm so that the 10-mm and 25-mm devices correspond to approximately one half and three times the half wavelength, respectively. Note that if shear lag effects are accounted for in the transducer, so that its effective dimension is slightly smaller than its nominal dimension (on the order of 15%), then the ratios would be in better agreement as observed in the experiment. Similarly at 125 kHz, the A_0 mode wavelength is ~14 mm, which makes the ratio of mode wavelength to transducer dimension close to 0.5. Furthermore, note that the wavelength at 150 kHz is equal to ~12.5 mm so that the 25-mm segment is expected to minimize the induced displacements as it is equal to twice the wavelength. While this is not exactly observed, note that there is a local minimum at this frequency.

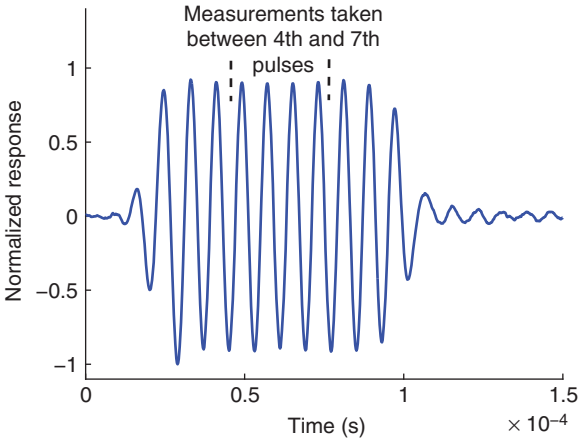

Figure 11. *Sample response measured with laser vibrometer for 10-cycle sinusoidal excitation at 125 kHz for 10 mm segment.*

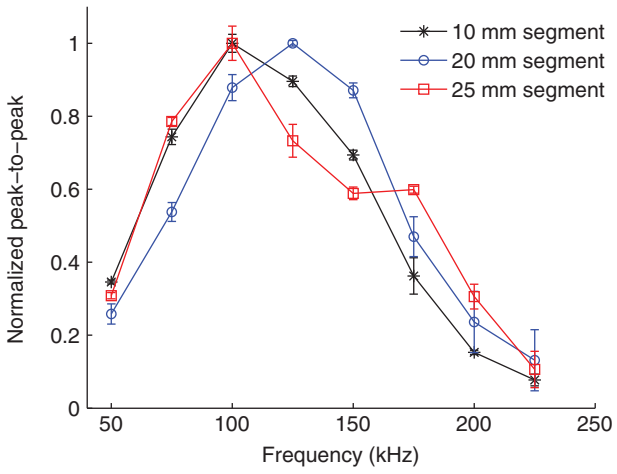

Figure 12. *Comparison of peak-to-peak amplitudes measured with laser vibrometer under near harmonic excitation conditions for various segments.*

These results provide a preliminary demonstration that the variable-length transducer can preferentially excite specific modes when sized according to the desired wavelength. The following subsection provides a detailed study on the effectiveness of the variable-length device in attaining different mode transmission and sensing ratios.

Sensor-based Experiments

The objective of this section is to evaluate the performance of the variable-length device in selectively exciting symmetric and antisymmetric modes at different frequencies. In this case, the GW field was recorded using a circular 5-mm diameter piezoelectric wafer bonded 12 cm away from the edge of the transducer along its centerline, as shown in Figure 13. This distance was selected as a good compromise among several factors. First, there must be sufficient distance between the actuator and sensor to allow the modes to separate due to their different group velocities. Similarly, the sensor must not be placed too far from the transducer as this would result in the amplitudes being unnecessarily attenuated and in boundary reflections interfering with the GW pulses. A 3.5-cycle Hann-modulated toneburst was used as the excitation signal in this case. The apparatus used to generate the pulse as well as the input voltages were similar to those in the previous set of experiments. The sensor data were recorded using a digital oscilloscope (Agilent Infinuum 54831DSO) with a sampling rate of 5 million samples per second. The sensor signals were post-processed by removing constant and linear trends and passed through a fourth-order Butterworth band-pass filter. The frequency band-pass was selected based on the center frequency of excitation and the number of cycles in the modulation window. While 128 averages were collected at each frequency tested, the standard deviation provided by the oscilloscope

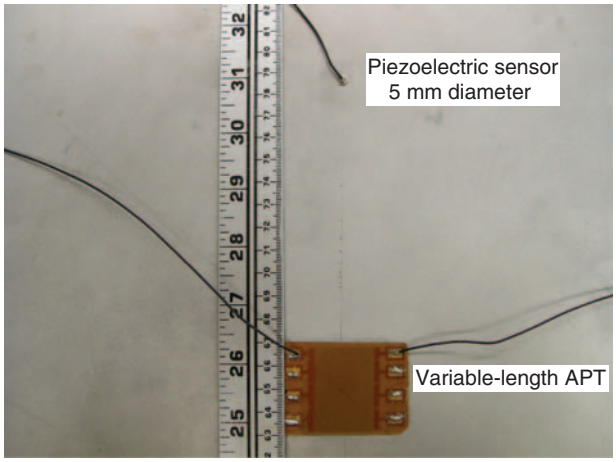

Figure 13. *Placement of the piezoceramic sensor relative to the variable-length APT on the substrate's surface.*

corresponded to the peak-to-peak amplitude of the entire signal, and it was therefore not used in the results as there were contributions from electromagnetic interference (EMI), as well as the propagating GW modes. Instead, over the large number of averages, it was observed that the standard deviation corresponded to at most 5% of the peak-to-peak amplitude. Consequently, the following convention was adopted for reporting the experimental error: When the specific mode under consideration had a dominant contribution in the signal, its error was assigned to be 5% of its peak-to-peak value. Conversely, when the contribution had to be manually tracked based on wave speeds, the error was raised to 15% of the peak-to-peak value. Considering the large number of averages taken, the error convention is expected to provide conservative estimates. For the transmission ratio, the error was computed using suitable error propagation equations.

Figures 14 and 15 show sample time domain signals recorded with the sensor at frequencies where the A_0 and S_0 modes are dominant, respectively. Similar measurements were recorded over a large range of frequencies and the peak-to-peak amplitude of each mode was recorded for each segment of the variable-length transducer. Sample results for the frequency response of these segments are shown in Figure 16. Note that, as expected, the A_0 mode is dominant at low frequencies, while the S_0 mode contribution increases at higher frequencies. In this case, however, the metric of interest is the ratio of S_0 to A_0 transmission attainable with each device. This ratio is used as a measure of the selectivity the transducer in GW generation. Figure 17 shows the comparison of this transmission ratio as a function of frequency for all the segments in the variable-length device, including the individual 5-mm segment needed to obtain the 25-mm dimension, in dB scale. From the figure it is clear that the smallest actuator has a lower transmission ratio

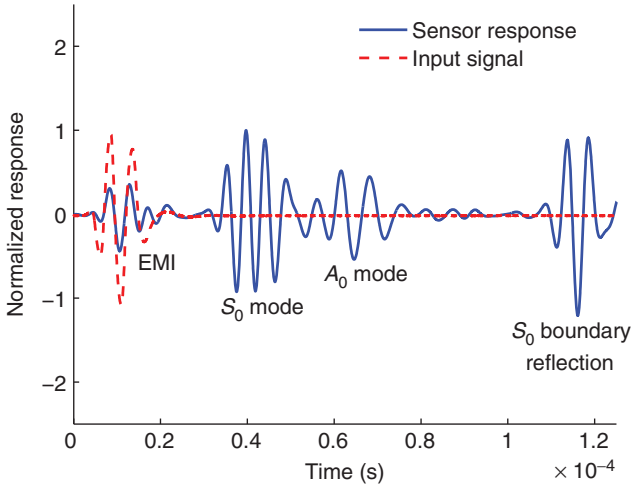

Figure 15. *Sample signal recorded with piezo sensor when S_0 mode is dominant using the 10 mm segment at 200 kHz.*

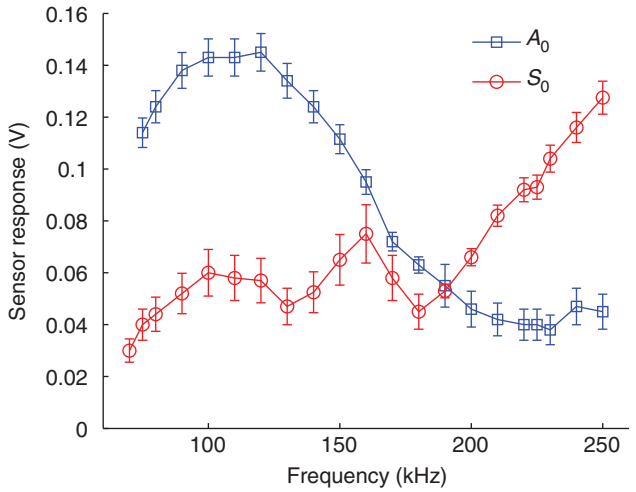

Figure 16. *Sample frequency response recorded for 20 mm segment using the piezoelectric sensor.*

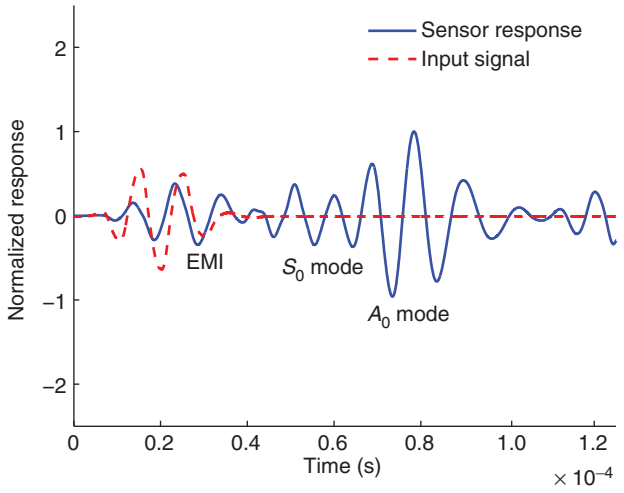

Figure 14. *Sample signal recorded with piezo sensor when A_0 mode is dominant using the 10 mm segment at 100 kHz.*

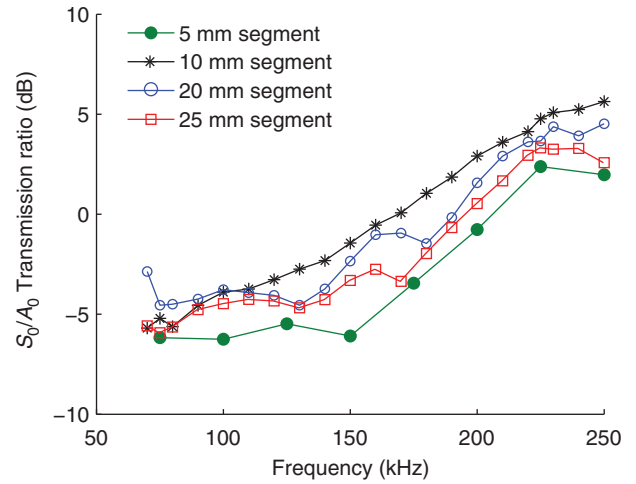

Figure 17. *Summary of S_0/A_0 transmission ratio as a function of frequency and transducer dimension.*

(S_0/A_0) over a wider frequency range due to the shorter wavelength of the antisymmetric mode, whose value decreases from ~18 mm at 75 kHz to 12 mm at 150 kHz. Similarly, the S_0 mode wavelength is very large in this frequency region (from 70 mm at 75 kHz to 35 mm at 150 kHz) so that the transducer is small enough to excite it in a weaker manner. The importance of this particular segment is that it would allow for surface damage inspection (e.g., surface cracks) using the A_0 mode in a nearly pure manner over a relatively large range of wavelengths.

As previously discussed, the 10-mm segment was selected so as to obtain a small S_0/A_0 transmission ratio at lower frequencies and a maximum transmission ratio in the neighborhood of 225 kHz (720 kHz mm). The results show that, until 100 kHz, this transducer dimension produces the lowest transmission ratio (along with the 25-mm segment) except for the 5-mm segment for the reasons discussed previously. Similarly, it can be observed that this segment produces the largest S_0/A_0 transmission ratio attainable with the entire transducer at higher frequencies as a result of its wavelength being close to half the wavelength of the S_0 mode in that region. Note that in this case, unlike other segments, the transmission ratio is expected to continue to increase with higher frequencies. While the wavelengths corresponding to the S_0 mode in this region are still relatively large, the results illustrate that by using a variable-length device the peak transmission ratios can be tailored to occur at specific frequencies, according to the wavelength desired. Finally, the 25-mm transducer was designed so as to maximize the transmission of the A_0 mode at 225 kHz (which is maximized by the 10-mm segment). The results illustrate that for this transducer dimension, the S_0/A_0 ratio is the lowest in all overall device, except for the 5-mm segment. It is important to emphasize once more the advantage offered by the variable-length capability of the transducer. Note that for the particular combination of parameters selected in this experimental demonstration, the largest improvement in mode purity occurs for the A_0 mode at 150 kHz. At this frequency, using the 5-mm segment yields a gain of ~4.6 dB relative to the 10-mm segment. This indicates that due to the ability of the device to electrically vary its length, the wavelength of the A_0 mode can be exploited for damage detection at this frequency without compromising, for instance, on the purity of the S_0 mode at 225 kHz. This illustrates the usefulness of the transducer, as different wavelengths can be selectively excited using a single, compact device.

During the selection of the transducer dimensions, the points chosen predicted a very low mode ratio at different frequencies, in fact lower than what is actually observed in the experiment. This observation is due to the inherent property of the substrate to have better excitability for each mode in different frequency-thickness ranges. Therefore, attempting to maximize the transmission of the S_0 mode at lower frequencies by selecting a dimension where the predicted A_0 excitation is minimal (or even zero) will only result in a higher S_0/A_0 ratio than otherwise possible. However, the A_0 mode will still be dominant. A second important observation is that in real applications, the specimens under inspection are excited with signals that contain a finite frequency bandwidth (typically a modulated toneburst), and therefore the center frequency, used in the transducer sizing, will not represent the only contribution. A possible future direction for development is the linkage between the excitation signal and the transducer dimension to generate a design that will result in a desired ratio once accounting for all frequency contributions.

The selectivity attainable when the variable-length device was used as a sensor was also evaluated. In this case, a circular piezoelectric wafer with a diameter of 16-mm was bonded on the surface of the plate, at 12 cm from the edge of the transducer as in the previous case, to act as a GW emitter. Due to the presence of additional sensors, the actuator was bonded on the opposite surface of the plate, as shown in Figure 18. In this set of experiments, the use of the amplifier was not necessary and the peak-to-peak voltage input was maintained at 18 V. A total of 64 averages were taken at each frequency, and due to similar considerations, the same error convention as in the actuator tests was adopted.

The results, shown in Figure 19, indicate that, when used as a sensor, the transducer preferentially senses the symmetric mode. This is likely due to its operation under the 3-3 piezoelectric effect which makes the transducer mostly sensitive to in-plane strains. This may be responsible for the larger S_0/A_0 sensing ratios observed in this case in contrast to the lower ratios observed for the transmission ratio. Note, however, that the peaks where the transmission ratios occur are not a function of the sensor dimension, but instead of the emitting transducer.

The trends observed when the device was used as an actuator are also present in this case. For instance, the 20-mm segment was designed to maximize the S_0 mode at 75 kHz, and it is observed that this device also has the largest S_0/A_0 sensing ratio at lower frequencies. Furthermore, the 10-mm device was selected to maximize the S_0 transmission at 225 kHz and minimize the A_0 transmission at 75 kHz. It can be observed that these trends are supported in the sensing results as well. Finally, the 25-mm device was sized so as to maximize the A_0 transmission at 225 kHz, and it can be seen that among all the combinations, except for the 5-mm device, this segment has the lowest S_0/A_0 sensing ratio.

These observations are equally important, as they indicate that independently of the source used, the sensor can be designed such that specific wavelengths are sensed more effectively. Note that in this case, the maximum performance improvement occurs at 75 kHz.

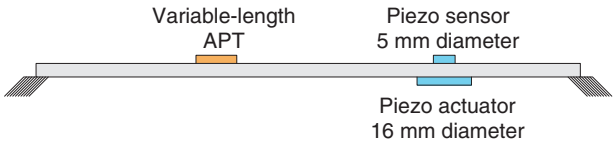

Figure 18. *Schematic illustrating the location of the piezoelectric wafer used as actuator for the sensing characterization of the variable-length transducer.*

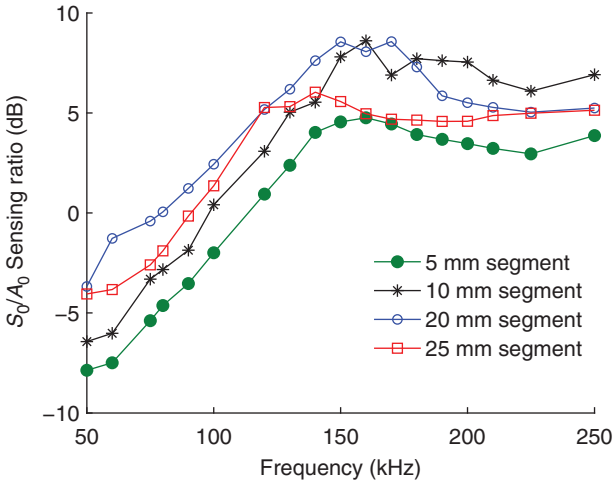

Figure 19. *Summary of S_0/A_0 sensing ratio as a function of frequency and transducer dimension.*

At this frequency, using the 5-mm segment yields a gain of ~6.2 dB relative to the 20-mm segment. Once again, this indicates that the wavelength at 75 kHz can be exploited without sacrificing the device sensitivity to the S_0 mode at 150 kHz, for instance. Using a sensor tuned for different wavelengths is particularly important in damage detection, where the reflection signals are typically small compared to the excitation pulses.

SUMMARY AND CONCLUSIONS

In this article, the design, manufacture, and testing of a variable-length anisotropic piezocomposite transducer were presented targeting SHM applications. The theoretical background necessary to determine the transducer dimensions, and their dependence on the mode wavelength were outlined. In particular, it was shown that the transducer dimension should be equal to integer multiples of the half-wavelength of the mode whose transmission is to be maximized and equal to integer multiples of the wavelength of the mode to be minimized. Using these results, the segments in the variable-length device were sized so as to maximize the transmission of individual modes at multiple frequencies. The variable-length effect was obtained through the design of an interdigitated electrode pattern with subdivisions for independent actuation and sensing. A combination of laser vibrometer and sensor-based experiments was used to characterize the transmission of the fundamental antisymmetric and symmetric Lamb modes in isotropic plates. It was shown that by using segments with different dimensions, the transmission and sensing ratios (S_0 to A_0 modes) could be tailored to peak at different frequencies. Furthermore, it was demonstrated that for the material system used a maximum mode purity gain of ~5 dB in transmission and 6 dB in sensing, relative to other elements in the variable-length device, could be obtained by appropriately selecting the transducer dimension based on the testing frequency. This is advantageous as it allows a single, compact device to interrogate a structure using a nearly pure mode at different wavelengths, which is expected to improve the damage sensitivity of the transducer. Directions for future work include sizing the individual segments according to the damage size to be detected, evaluating the variable-length effect in composite structures, and the design of variable-length transducers that account for the multiple frequencies contained in a typical excitation signal.

ACKNOWLEDGMENTS

The authors gratefully acknowledge Mr J. W. High and Dr R. G. Bryant, NASA Langley Research Center, and Dr W. Keats Wilkie, NASA Jet Propulsion Laboratory, for providing some of the piezoelectric materials used in this study. The assistance of Mr Edward Tang, Senior Engineer at the Lurie Nanofabrication Facility at the University of Michigan, in fabricating the electrodes for the piezocomposite transducer used in this study is greatly appreciated. This work was partly supported by the Air Force Office of Scientific Research under grants FA9550-06-1-0071 and FA9550-07-1-0522 with Dr Victor Giurgiutiu as the technical monitor. This work was also supported by the NASA Constellation University Institutes Project under grant Z634001, with Ms Claudia Meyer as the project manager.

REFERENCES

Alleyne, D. and Cawley, P. 1992. "The Interaction of Lamb Waves with Defects," *IEEE Transactions on Ultrasonics, Ferroelectrics, and Frequency Control*, 39(3):381–397.

Bent, A.A. and Hagood, N.W. 1995. "Anisotropic Actuation with Piezoelectric Fiber Composites," *Journal of Intelligent Materials Systems and Structures*, 6(3):338–349.

Chen, F. and Wilcox, P.D. 2007. "The Effect of Load on Guided Wave Propagation," *Ultrasonics*, 47(4):111–122.

Clarke, T. and Cawley, P. 2008. "Monitoring of Complex Structures Using Guided Waves," In: *Proceedings of the 4th European Workshop on Structural Health Monitoring*, Krakow, Poland.

Crawley, E.F. and de Luis, J. 1987. "Use of Piezoelectric Actuators as Elements of Intelligent Structures," *AIAA Journal*, 25(10): 1373–1385.

Diamanti, K., Hodgkinson, J.M. and Soutis, C. 2004. "Detection of Low-velocity Impact Damage in Composite Plates Using Lamb Waves," *Structural Health Monitoring*, 3(1):33–41.

Diamanti, K., Soutis, C. and Hodgkinson, J.M. 2005. "Non-destructive Inspection of Sandwich and Repaired Composite Laminated Structures," *Composites Science and Technology*, 65(3):2059–2067.

Diamanti, K., Soutis, C. and Hodgkinson, J.M. 2007. "Piezoelectric Transducer Arrangement for the Inspection of Large Composite Structures," *Composites A*, 38(4):1121–1130.

Diligent, O. and Lowe, M.J.S. 2005. "Reflection of the s_0 Lamb Mode from a Flat Bottom Circular Hole," *Journal of the Acoustical Society of America*, 118(5):2869–2879.

Fromme, P., Wilcox, P., Lowe, M. and Cawley, P. 2004. "On the Scattering and Mode Conversion of the A_0 Lamb Wave Mode at Circular Defects in Plates," *Review of Progress in QNDE*, 22A:142–149.

Graff, K. 1991. *Wave Motion in Elastic Solids*, Dover Publications, New York.

Konstantinidis, G., Drinkwater, B.W. and Wilcox, P.D. 2006. "The Temperature Stability of Guided Wave Structural Health Monitoring Systems," *Smart Materials and Structures*, 15(4): 967–976.

Lowe, M.J.S., Cawley, P., Kao, J.-Y. and Diligent, O. 2002. "The Low Frequency Reflection Characteristics of the Fundamental Antisymmetric Lamb Wave a_0 from a Rectangular Notch in a Plate," *Journal of the Acoustical Society of America*, 112(6): 2612–2622.

Monkhouse, R.S.C., Wilcox, P.D. and Cawley, P. 1997. "Flexible Interdigital PVDF Transducers for the Generation of Lamb Waves in Structures," *Ultrasonics*, 35(7):489–498.

Monkhouse, R.S.C., Wilcox, P.D., Lowe, M.J.S., Dalton, R.P. and Cawley, P. 2000. "The Rapid Monitoring of Structures Using Interdigital Lamb Wave Transducers," *Smart Materials and Structures*, 9(3):304–309.

Pavlakovic, B. and Lowe, M.J.S. 2007. Disperse Software Manual version 2.0.16d, Imperial College London, UK.

Pelts, S.P., Jiao, D. and Rose, J.L. 1996. "A Comb Transducer for Guided Wave Generation and Mode Selection," In: *Proceedings of the IEEE Ultrasonics Symposium*, Vol. 2, pp. 857–860.

Polytec PSV-400 Scanning Laser Vibrometer Hardware Manual, Polytec GmbH, 2007.

Raghavan, A. and Cesnik, C.E.S. 2005. "Finite-dimensional Piezoelectric Transducer Modeling for Guided Wave Based Structural Health Monitoring," *Smart Materials and Structures*, 14(6):1448–1461.

Raghavan, A. and Cesnik, C.E.S. 2007a. "Review of Guided-wave Based Structural Health Monitoring," *The Shock and Vibration Digest*, 39(2):91–114.

Raghavan, A. and Cesnik, C.E.S., 2007b, "Studies on Effects of Elevated Temperature for Guided-wave Structural Health Monitoring," In: *Proceedings of the 14th SPIE International Symposium on Smart Structures and Materials/NDE and Health Monitoring*, San Diego, CA.

Raghavan, A. and Cesnik, C.E.S. 2007c. "3-D Elasticity-based Modeling of Anisotropic Piezocomposite Transducers for Guided Wave Structural Health Monitoring," *Journal of Vibration and Acoustics*, 129(6):739–751.

Salas, K.I. and Cesnik, C.E.S. 2008a. "Design and Characterization of the CLoVER Transducer for Structural Health Monitoring," In: *Proceedings of the 15th SPIE International Symposium on Smart Structures and Materials/NDE and Health Monitoring*, San Diego CA.

Salas, K.I. and Cesnik, C.E.S. 2008b. "Guided Wave Experimentation using CLoVER Transducers for Structural Health Monitoring," In: *Proceedings of the 16thAIAA/ASME/AHS Adaptive Structures Conference*, Schaumburg, IL.

Salas, K.I. and Cesnik, C.E.S. 2009. "Guided Wave Excitation by a CLoVER Transducer: Theory and Experiments," *Smart Materials and Structures*, 18(7):075005.

Wilkie, W.K. and High, J.W. 2003. Method of Fabricating NASA-standard Macro-fiber Composite Piezoelectric Actuators, NASA Technical Report TR-2003-212427.

Williams, R.B. 2004. "Nonlinear Mechanical and Actuation Characterization of Piezoceramic Fiber Composites", PhD Thesis, Virginia Polytechnic Institute and State University, Blacksburg, VA.